Title
ENERGY-DISPERSIVE X-RAY FLOURESCENCE (EDXRF) ANALYSIS OF MAJOR, MINOR AND TRACE ELEMENTS FOR AN ANDESITE TUFF SEDIMENT, ARROYO HONDO, NORTHERN NEW MEXICO

Author
Shackley, M. Steven

Publication Date
2020-08-10

GEOARCHAEOLOGICAL XRF LAB
A GREEN SOLAR FACILITY

GEOARCHAEOLOGICAL X-RAY FLUORESCENCE SPECTROMETRY LABORATORY
8100 Wyoming Blvd., Ste M4-158 Albuquerque, NM 87113
USA

ENERGY-DISPERSIVE X-RAY FLOURESCENCE (EDXRF) ANALYSIS OF MAJOR, MINOR AND TRACE ELEMENTS FOR AN ANDESITE TUFF SEDIMENT, ARROYO HONDO, NORTHERN NEW MEXICO

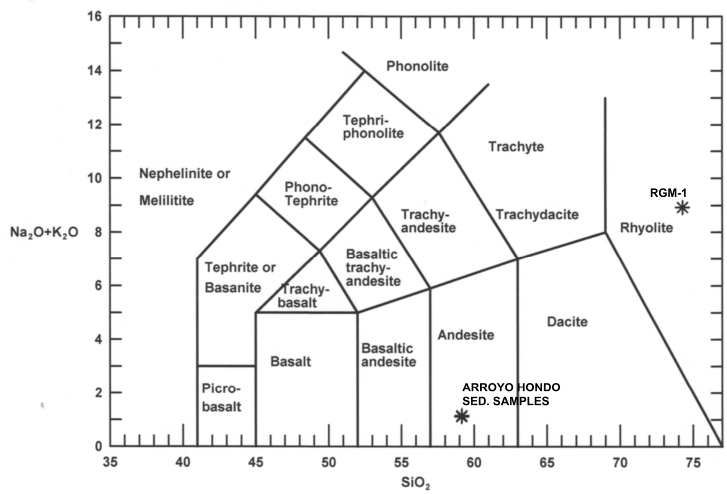

by

M. Steven Shackley, Ph.D., Director
Geoarchaeological XRF Laboratory
Albuquerque, New Mexico

Report Prepared for

Dr. Judith Habicht-Mauche
Department of Anthropology
University of California
Santa Cruz, California

10 August 2020

INTRODUCTION

The analysis here of a sediment sample from a tuff strata on the south slope of Arroyo Hondo directly below the northwest corner of Arroyo Hondo Pueblo is a low-alkali andesite tuff based on the elemental composition (see Table 1 and Figure 1). While the Turquoise Hill 7.5' Quadrangle where Arroyo Hondo resides has not been geologically mapped by the New Mexico Bureau of Geology and Mineral Resources StateMap section, the Santa Fe Quad to the northeast had been mapped (Read et al. 2000). The description of the Bishop Lodge Member of the Tesuque Formation that is present on the front of the Sangre de Cristo range in northern New Mexico appears similar to this rock and its environment (G. Smith in Read et al. 2000). A biotite $^{40}Ar/^{39}Ar$ date of 30.45 +0.16 Ma was obtained by the NMGRL for the pumice-fall bed that closely describes the sediment in this analysis: "distinctly volcaniclastic, composed of white tuffaceous mudstone and gray, conglomeratic volcanic-lithic sandstones" and I would add capped by a partly indurated ashy-horizon, possibly mudstone (Smith in Read et al. 2000: 9-10). I have only examined a small portion of the sediment, however. A more thorough analysis will follow.

According to Habicht-Mauche, Santa Fe Black-on-white, var. Pindi contains "medium to coarse pumiceous ash" some with "clear and pink glass shards" which very well could be derived from the sedimentary member here (1993:131-135). Optical petrography could aid in the determination of the relationship between this sediment and that used in Santa Fe Black-on-white temper. Examination of the sample analyzed here under 30X did reveal some quartz, biotite, and glass shards, but that would be typical in any andesite tuff.

LABORATORY SAMPLING, ANALYSIS AND INSTRUMENTATION

All samples are analyzed whole. Two splits of the sample were analyzed and the results are very similar (Table 1 and Figure 1). Each solid sample was subjected to high pressure air to remove any dust matrix from the rock, particularly with vesicular samples.

The results presented here are quantitative in that they are derived from "filtered" intensity values ratioed to the appropriate x-ray continuum regions through a least squares fitting formula rather than plotting the proportions of the net intensities in a ternary system (McCarthy and Schamber 1981; Schamber 1977). Or more essentially, these data through the comparative analysis of international rock standards, allow for inter-instrument comparison with a predictable degree of certainty (Hampel 1984; Shackley 2011).

All analyses for this study were conducted on a ThermoScientific *Quant'X* EDXRF spectrometer, located at the Geoarchaeological XRF Laboratory, Albuquerque, New Mexico. The spectrometer is equipped with a thermoelectrically Peltier cooled solid-state Si(Li) X-ray detector, with a 50 kV, 50 W, ultra-high-flux end window bremsstrahlung, Rh target X-ray tube and a 76 μm (3 mil) beryllium (Be) window (air cooled), that runs on a power supply operating from 4-50 kV/0.02-1.0 mA at 0.02 increments. The spectrometer is equipped with a 200 l min^{-1} Edwards vacuum pump, allowing for the analysis of lower-atomic-weight elements between sodium (Na) and titanium (Ti). Data acquisition is accomplished with a pulse processor and an analogue-to-digital converter. Elemental composition is identified with digital filter background removal, least squares empirical peak deconvolution, gross peak intensities and net peak intensities above background.

The data from the WinTrace™ software were translated directly into Excel for Windows software for manipulation and on into IGPET ver. 2013 for plotting (Carr and Gazel 2017). In order to evaluate these quantitative determinations, machine data were compared to measurements of known standards during each run. RGM-1 a USGS rhyolite standard was analyzed during each run of ≤19 samples. The USGS recommended values for RGM-1 are included in Table 1. Trace element data exhibited in Table 1 are reported in weight percent and parts per million (ppm), a quantitative measure by weight as noted.

Trace Element Analysis

In the analysis of mid Zb condition elements Ti-Nb, and high Zb Pb, Th, the x-ray tube is operated at 30 kV, using a 0.05 mm (medium) Pd primary beam filter in an air path at 100 seconds livetime to generate x-ray intensity $K\alpha_1$-line data for elements manganese (Mn), cobalt (Co), nickel (Ni), copper, (Cu), zinc, (Zn), gallium (Ga), rubidium (Rb), strontium (Sr), yttrium (Y), zirconium (Zr), niobium (Nb), and $L\alpha_1$ data for lead (Pb), and thorium (Th). Trace element intensities were converted to concentration estimates by employing a linear calibration line ratioed to the Compton scatter established for each element from the analysis of international rock standards certified by the National Institute of Standards and Technology (NIST), the US. Geological Survey (USGS), Canadian Centre for Mineral and Energy Technology, and the Centre de Recherches Pétrographiques et Géochimiques in France (Govindaraju 1994). Line fitting is linear (XML) for all elements. When barium (Ba) and cerium (Ce) is analyzed in the High Zb condition, the Rh tube is operated at 50 kV and up to 1.0 mA, ratioed to the bremsstrahlung region (see Davis 2011; Shackley 2011). Further details concerning the petrological choice of these elements in Southwest volcanic rocks is available in Shackley (1988, 1995, 2005, 2011; also Mahood and Stimac 1991; and Hughes and Smith 1993; Shackley et al. 2016, 2018). Nineteen specific pressed powder standards are used for the best fit regression calibration for elements Ti-Nb, Pb, Th, Ba, and Ce, and include G-2 (basalt), AGV-2 (andesite), GSP-2 (granodiorite), SY-2 (syenite), BHVO-2 (hawaiite), STM-1 (syenite), QLO-1 (quartz latite), RGM-1 (obsidian), W-2 (diabase), BIR-1 (basalt), SDC-1 (mica schist), TLM-1 (tonalite), SCO-1 (shale), NOD-A-1 and NOD-P-1 (manganese) all US Geological Survey standards, NIST-278 (obsidian), U.S. National Institute of Standards and Technology, BE-N (basalt) from the Centre de Recherches Pétrographiques et Géochimiques in France, and JR-1 and JR-2 (obsidian) from the Geological Survey of Japan (Govindaraju 1994).

Major and Minor Oxide Analysis

Analysis of the major oxides of Na, Mg, Al, Si, K, Ca, Ti, and Fe is performed under the multiple conditions elucidated below. This fundamental parameter analysis (theoretical with standards), while not as accurate as destructive analyses (pressed powder and fusion disks) most elements are usually ≤ 1% of actual, based on the analysis of the USGS RGM-1 rhyolite standard (Table 1). The fundamental parameter (theoretical) method is run under conditions commensurate with the elements of interest and calibrated with 11 USGS standards (RGM-1, rhyolite; AGV-2, andesite; BHVO-1, hawaiite; BIR-1, basalt; G-2, granite; GSP-2, granodiorite; BCR-2, basalt; W-2, diabase; QLO-1, quartz latite; STM-1, syenite), and one Japanese Geological Survey rhyolite standard (JR-1).

Conditions Of Fundamental Parameter Analysis[1]:

Low Za (Na, Mg, Al, Si, P)

Voltage	6 kV	Current	Auto[2]
Livetime	100 seconds	Counts Limit	0
Filter	No Filter	Atmosphere	Vacuum
Maximum Energy	10 keV	Count Rate	Low

Mid Zb (K, Ca, Ti, V, Cr, Mn, Fe)

Voltage	32 kV	Current	Auto
Livetime	100 seconds	Counts Limit	0
Filter	Pd (0.06 mm)	Atmosphere	Vacuum
Maximum Energy	40 keV	Count Rate	Medium

High □b (Sn, Sb, □a, Ag, Cd)

Voltage	50 kV	Current	Auto
Livetime	100 seconds	Counts Limit	0
Filter	Cu (0.559 mm)	Atmosphere	Vacuum
Maximum Energy	40 keV	Count Rate	High

□ow □b (S, Cl, □, Ca)

Voltage	8 kV	Current	Auto
Livetime	100 seconds	Counts Limit	0
Filter	Cellulose (0.06 mm)	Atmosphere	Vacuum
Maximum Energy	10 keV	Count Rate	Low

[1] Multiple conditions designed to ameliorate peak overlap identified with digital filter background removal, least squares empirical peak deconvolution, gross peak intensities and net peak intensities above background.

[2] Current is set automatically based on the mass absorption coefficient.

REFERENCES CITED

Carr, MJ, and E Gazel, 2017, Igpet software for modeling igneous processes: examples of application using the open educational version. *Miner Petrol* 111:283–289.

Davis, M.K., Jackson, T.L., Shackley, M.S., Teague, T., and Hampel J., [new introduction by M.S. Shackley], 2011, Factors affecting the energy-dispersive x-ray fluorescence (EDXRF) analysis of archaeological obsidian, *in* Shackley, M.S., ed., X-Ray Fluorescence Spectrometry (XRF) in Geoarchaeology: New York, Springer Publishing, p. 45–64.

Govindaraju, K., 1994, Compilation of working values and sample description for 383 geostandards: Geostandards Newsletter v. 18 (special issue), 158 p.

Habicht-Mauche, J. 1993, *The Pottery from Arroyo Hondo Pueblo, New Mexico: Tribalization and Trade in the Northern Rio Grande.* Arroyo Hondo Archaeological Series 8, School of American Research Press, Santa Fe.

Hampel, J.H., 1984, Technical considerations in x-ray fluorescence analysis of obsidian; *in* R.E. Hughes ed., Obsidian Studies in the Great Basin: Berkeley, Contributions of the University of California Archaeological Research Facility 45, p. 21–25.

Hildreth, W., 1981, Gradients in Silicic Magma Chambers: Implications for Lithospheric Magmatism. *Journal of Geophysical Research* 86:10153-10192.

Hughes, R. E., and R. L. Smith, 1993, Archaeology, geology, and geochemistry in obsidian provenance studies. *In Scale on Archaeological and Geoscientific Perspectives*, edited by J.K. Stein and A.R. Linse, pp. 79-91. Geological Society of America Special Paper 283.

Le Maitre, R.; Bateman, P.; Dudek, A.; Keller, J.; Lameyre, J.; Le Bas, M.; Sabine, P.; Schmid, R.; Sorensen, H.; Streckeisen, A.; Woolley, A.; Zanettin, B. 1989, A classification of igneous rocks and glossary of terms: Recommendations of the International Union of Geological Sciences Subcommission on the Systematics of igneous rocks (Le Maitre, R.W.; editor). Blackwell, 193 p. Oxford.

Mahood, Gail A., and James A. Stimac, 1990, Trace-element partitioning in pantellerites and trachytes. *Geochemica et Cosmochimica Acta* 54:2257-2276.

McCarthy, J.J., and F.H. Schamber, 1981, Least-squares fit with digital filter: a status report. In *Energy Dispersive X-ray Spectrometry*, edited by K.F.J. Heinrich, D.E. Newbury, R.L. Myklebust, and C.E. Fiori, pp. 273-296. National Bureau of Standards Special Publication 604, Washington, D.C.

Read, A.S., Koning, D.J., Smith, G.A., Ralser, S., Rodgers, J.B., and Bauer, P.A. 2000, *Report accompanying* Geologic map of Santa Fe Quadrangle, Santa Fe County, New Mexico. Open-file Geologic Map OF-GM 032. New Mexico Bureau of Geology and Mineral Resources, Socorro.

Schamber, F.H., 1977, A modification of the linear least-squares fitting method which provides continuum suppression. In *X-ray Fluorescence Analysis of Environmental Samples*, edited by T.G. Dzubay, pp. 241-257. Ann Arbor Science Publishers.

Shackley, M.S., 1988, Sources of archaeological obsidian in the Southwest: an archaeological, petrological, and geochemical study. *American Antiquity* 53:752-772.

Shackley, M. S.,1995, Sources of archaeological obsidian in the greater American Southwest: an update and quantitative analysis. *American Antiquity* 60(3):531-551.

Shackley, M.S., 2005, *Obsidian: Geology and Archaeology in the North American Southwest*. University of Arizona Press, Tucson.

Shackley, M.S., 2011, An introduction to x-ray fluorescence (XRF) analysis in archaeology. In *X-Ray Fluorescence Spectrometry (XRF) in Geoarchaeology*, M.S. Shackley (Ed.), pp. 7-44. Springer, New York.

Shackley, M.S., F. Goff, and S.G. Dolan, 2016, Geologic origin of the source of Bearhead rhyolite (Paliza Canyon) obsidian, Jemez Mountains, Northern New Mexico. *New Mexico Geology* 38:52-62.

Shackley, M.S., L.E. Morgan, and D. Pyle, 2018, Elemental, isotopic, and geochronological variability in Mogollon-Datil Volcanic Province archaeological obsidian, southwestern USA: solving issues of inter-source discrimination. *Geoarchaeology* 33:486-497.

Table 1. Non-normalized major, minor and trace elemental concentrations for the rock samples, USGS RGM-1, and USGS RGM-1 recommended values . All measurements in weight percent (%) or parts per million (ppm) as noted (see http://swxrflab.net/anlysis.htm).

Sample	Na_2O	MgO	Al_2O_3	SiO_2	K_2O	CaO	TiO_2	MnO	Fe_2O_3	Σ				
	%	%	%	%	%	%	%	%	%					
ARROYOHONDO1	0.52	28.64	2.36	58.86	0.59	7.96	0.02	0.05	0.56	99.57				
ARROYO HONDO2	0.59	28.77	2.27	58.86	0.56	7.89	0.03	0.05	0.51	99.54				
RGM1-S4	3.94	0.00	12.91	73.94	4.95	1.43	0.30	0.04	2.25	99.76				
RGM-1 recommended σ	4.07	0.28	13.70	73.40	4.30	1.15	0.27	0.04	1.86					
	Cl	Ni	Cu	Zn	Ga	Rb	Sr	Y	Zr	Nb	Ba	Ce	Pb	Th
	ppm	ppm	ppm	ppm	ppm	ppm	ppm	ppm	ppm	ppm	ppm	ppm	ppm	ppm
ARROYOHONDO1	420	17	47	39	11	8	777	8	47	3	2505	64	4	4
ARROYOHONDO2	306	19	47	28	10	16	769	11	71	9	1880	43	10	4
RGM1-S4	484	16	15	46	17	148	104	25	223	14	799	33	24	22
RGM-1 recommended σ	510	nr	12	32	15	150	110	25	220	9	810	47	24	15

nr = not reported

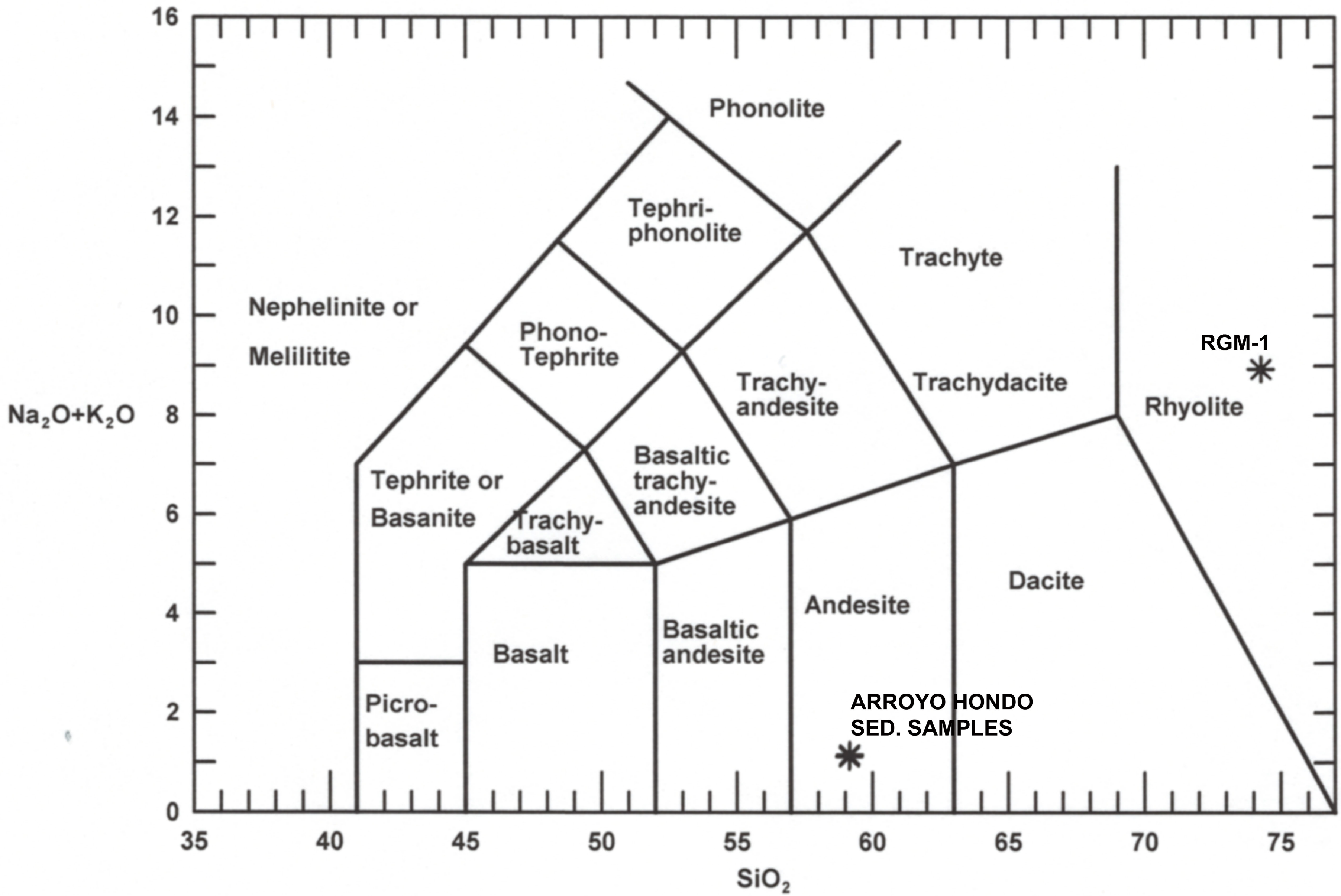

Figure 1. TAS plot of the Arroyo Hondo sediment samples and USGS RGM-1 (Le Maitre et al. 1989).